Ultrasonics Sonochemistry 73 (2021) 105494

Contents lists available at ScienceDirect

Ultrasonics Sonochemistry

journal homepage: www.elsevier.com/locate/ultson

Sensitization of nerve cells to ultrasound stimulation through Piezo1-targeted microbubbles

Xuelian Shen [a], Zhuqing Song [b], Erjiao Xu [a], Jun Zhou [c,*], Fei Yan [d,*]

[a] Department of Medical Ultrasonics, The Eighth Affiliated Hospital, Sun Yat-sen University, Shenzhen 518033, China
[b] Department of Breast Surgery, Peking University Shenzhen Hospital, Shenzhen 518036, China
[c] Department of Ultrasound, The First College of Clinical Medical Science, China Three Gorges University, Yi Chang, Hubei 443000, China
[d] CAS Key Laboratory of Quantitative Engineering Biology, Shenzhen Institute of Synthetic Biology, Shenzhen Institutes of Advanced Technology, Chinese Academy of Sciences, Shenzhen 518055, China

ARTICLE INFO

Keywords:
Neuromodulation
Ultrasound stimulation
Microbubbles
Piezo1
Ca^{2+} transients

ABSTRACT

Neuromodulation by ultrasound (US) has recently drawn considerable attention due to its great advantages in noninvasiveness, high penetrability across the skull and highly focusable acoustic energy. However, the mechanisms and safety from US irradiation still remain less understood. Recently, documents revealed Piezo1, a mechanosensitive cation channel, plays key role in converting mechanical stimuli from US through its trimeric propeller-like structure. Here, we developed a Piezo1-targeted microbubble (PTMB) which can bind to the extracellular domains of Piezo1 channel. Due to the higher responsiveness of bubbles to mechanical stimuli from US, significantly lower US energy for these PTMB-binding cells may be needed to open these mechanosensitive channels. Our results showed US energy at 0.03 MPa of peak negative pressure can achieve an equivalent level of cytoplasmic Ca^{2+} transients which generally needs 0.17 MPa US intensity for the control cells. Cytoplasmic Ca^{2+} elevations were greatly reduced by chelating extracellular calcium ions or using the cationic ion channel inhibitors, confirming that US-mediated calcium influx are dependent on the Piezo1 channels. No bubble destruction and obvious temperature increase were observed during the US exposure, indicating cavitation and heating effects hardly participate in the process of Ca^{2+} transients. In conclusion, our study provides a novel strategy to sensitize the response of nerve cells to US stimulation, which makes it safer application for US-mediated neuromodulation in the future.

1. Introduction

Neuromodulation mediated by US has recently drawn considerable attention due to its apparent advantages such as noninvasiveness. Great application potentials are disclosed as a powerful tool used for brain function researches and for treating neurological or psychiatric diseases [1–3]. Although some similar techniques such as electrical stimulation, optical genetic technology, and magnetic stimulation have successfully applied to modulate nerve activity, each one has their own drawbacks [4–6]. For example, deep brain stimulation (DBS) with electrical impulses shows its efficacy in some neurological disorders, including Parkinson's disease, essential tremor, epilepsy, and dystonia. Optical genetic technology is considered to be a powerful tool in understanding of neural circuit. But both DBS and optogenetic approaches are invasive. Magnetic stimulation is noninvasive but its focusing performance is relatively poor. Therefore, it is necessary to develop a new brain stimulation method which can realize the noninvasive and targeted neuromodulation.

US is a sound wave with greater frequency than the human auditory detection level (>20 KHz), generating mechanical wave by the vibration due to the compression and expansion of the medium from sound source and inducing various acoustic effects such as volatility, mechanical effects and thermal effects, which have widely applications in biomedicine [7,8]. Recent studies have revealed that mechanical effects from US show significant potential in the neuromodulation. Due to its ability to noninvasively propagate through bone and other tissues in a focused manner with high spatial resolution, US provides a powerful tool for the precise modulation of neural circuit activity and brain research. In 2014, Legon et al first found transcranial focused ultrasound (tFUS) with a low frequency can focus into the human primary somatosensory cortex (S1)

* Corresponding authors.
E-mail addresses: zjsts8@163.com (J. Zhou), fei.yan@siat.ac.cn (F. Yan).

https://doi.org/10.1016/j.ultsonch.2021.105494
Received 24 October 2020; Received in revised form 19 January 2021; Accepted 5 February 2021
Available online 13 February 2021
1350-4177/© 2021 The Authors. Published by Elsevier B.V. This is an open access article under the CC BY-NC-ND license (http://creativecommons.org/licenses/by-nc-nd/4.0/).

and improve the ability of sensory discrimination abilities [9]. Lee et al reported FUS sonication of the primary visual cortex in humans, resulting in elicited activation not only from the sonicated brain area, but also from the network of regions involved in visual and higher-order cognitive processes [10].

Although the mechanisms of ultrasonic neuromodulation are still unclear, numerous studies have shown that US can stimulate neurons through activating the cationic ion channels in the neuronal cell membrane, resulting in some cationic ions to flow towards the inside of the cells and to excite these cells [8]. For example, Tyler found that US can activate the sodium channels and calcium channels on the neurons and trigger action potential [11]. To explain the effects of US on neuronal activity, several different hypotheses have been proposed. Among them, the most important one is the role of acoustic radiation force in neuromodulation. Acoustic radiation force from US irradiation may induce lipid bilayer tension and alter the membrane potential through ion flow inside and outside the membrane, and the changes of ion concentrations further excite cellular activity [12]. Similar with voltage-gated channels and ligand-gated channels, some transmembrane proteins which possess mechanically sensitive properties to modulate ion channels were found.

To date, there are two mechanosensitive ion channels (Piezo1 and Piezo2) discovered on the cell membrane that can induces mechanically activated currents in cells [13]. Piezo1 is considered to be essential for the response of cells to mechanics, such as tactile, auditory, ontological sensory. Recent study from the cryo-electron microscopy structure revealed that Piezo1 forms a trimeric propeller-like structure, with the extracellular domains resembling three distal blades and a central cap. The flexible extracellular blade domains are connected to the central intracellular domain by three long beam-like structures, suggesting that Piezo1 may use its peripheral regions as force sensors to gate the central ion-conducting pore [14]. Qiu Z et al further found that Piezo1 plays an important role in mediating the in vitro effects of US in mouse primary cortical neurons and a neuronal cell line, showing that US alone could activate heterologous and endogenous Piezo1 through initiating calcium influx in primary neurons [15]. Considering that microbubbles (MBs) possess a high sensitivity to US, we hypothesized that Piezo1-targeted MBs (PTMB) would enhance the stimulation effect of US on neuromodulation. Before US stimulation, extracellular calcium concentration is higher than intracellular calcium concentration and the Piezo1 channel (PTMB can attach to the channel via receptor-ligand interaction) on the cell membrane is closed. Upon receiving US stimulation, Piezo1 channel would be pulled open by PTMB and the extracellular Ca^{2+} ions would flow into the cells (Scheme 1).

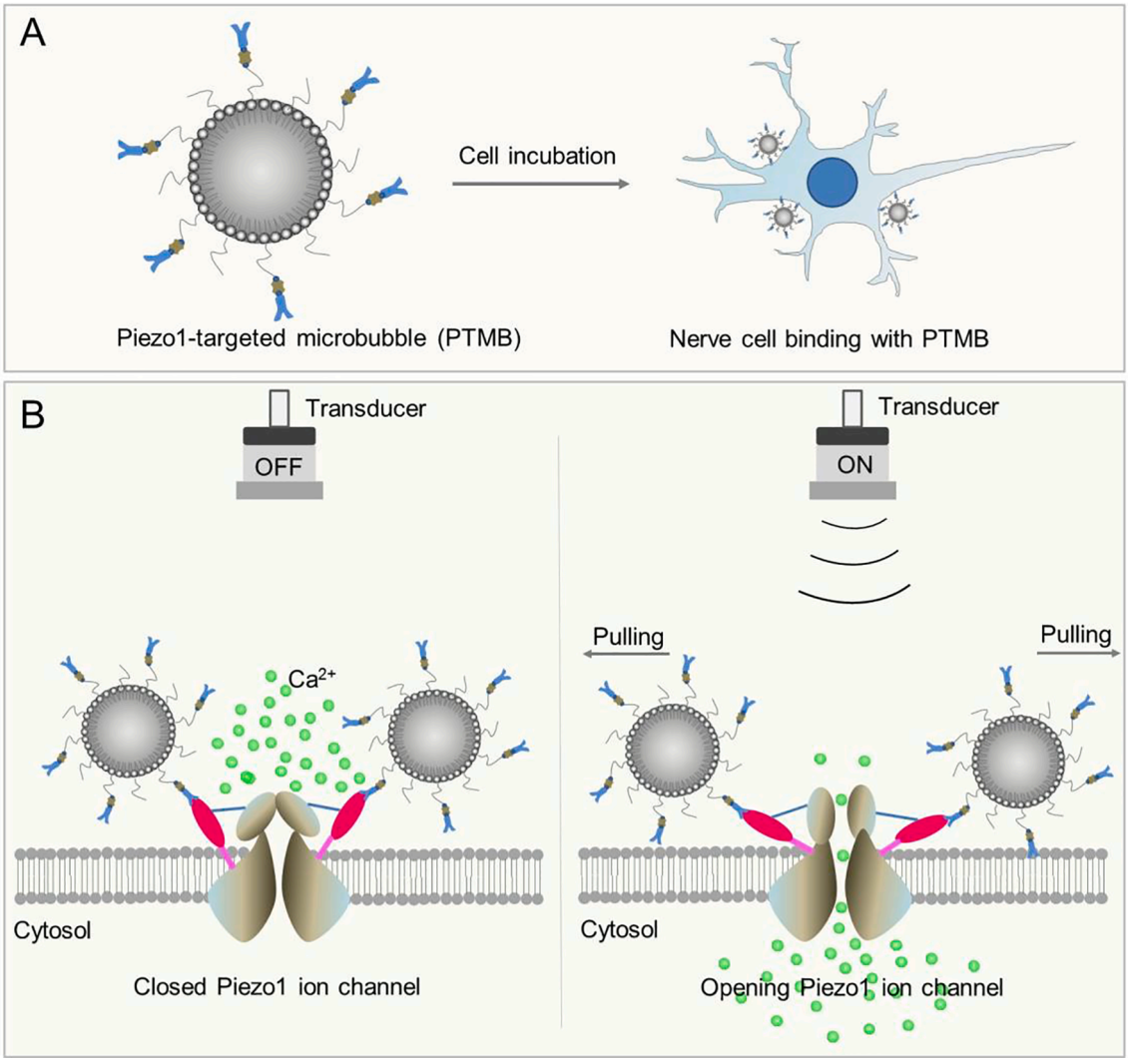

Scheme 1. The diagram of PTMB binding to the cells and the enhanced calcium influx by US stimulation. PTMB was incubated with nerve cells, resulting in the binding of Piezo1-MBs to the Piezo1 channel. Before US stimulation, extracellular calcium concentration is higher than intracellular calcium concentration and the Piezo1 channel to which PTMB attached via receptor-ligand binding on the cell membrane is closed. US stimulation lead to the opening of Piezo1 channel, followed by extracellular calcium flowing into the cells.

2. Materials and methods

2.1. Preparation of Piezo1-MBs

1, 2-distearoyl-*sn*-glycero-3-phosphatidylcholine (DSPC), 1, 2-distearoyl-*sn*-glycero-3-phosphoethanolamine-N-[Methoxy (Polyethylene glycol)-2000] (DSPE-PEG2000) and 1, 2-distearoyl-*sn*-glycero-3-phosphoethanolamine-N-[Biotinyl (Polyethylene Glycol)-2000] (DSPE-PEG2000-Biotin) were purchased from Avanti Polar Lipids, Inc. (Alabaster, AL, USA). Briefly, the DSPC: DSPE-PEG2000: DSPE-PEG2000-biotin with molar ratios (9: 0.5: 0.5) were added and blended in chloroform. Afterward, the solvent was removed under nitrogen flow at room temperature. The dried phospholipid blends were hydrated by ultrasonic bath at 60 °C with 5 mL of degassed Tris buffer solution (containing 10% glycerol and 10% propylene glycol, pH 7.4). Next, we divided the phospholipid solution into vials. The air in the phospholipid solution was replaced with perfluoropropane (C_3F_8; Flura, Newport, TN, USA) through our self-made device. Finally, the vial was placed on an oscillator (A. max AM-1 Capsule Mixer, Monitex, USA) for mechanical oscillation for 45 s to obtain the biotinylated MBs.

The biotinylated MBs were used to prepare the Piezo1-MBs via avidin-biotin linkage. In brief, MBs were washed with PBS solution two times in a bucket rotor centrifuge at 400 g for 4 min to remove excess unincorporated lipids from the MBs. 30 μg of avidin (Sigma-Aldrich, USA) per 10^8 MBs was then added to the washed MB dispersion. Followed by the incubation for 30 min at room temperature, the MBs were washed two times to remove unreacted avidin, and then incubated at room temperature with 3 μg of biotinylated anti-Piezo1 or IgG antibodies (Novus Biologicals, USA) for another 30 min. Free antibodies were removed through washing with PBS. Particle size, size distribution and concentration of targeted MBs were determined using an optical particle counter with a 0.5 μm diameter detection limit (Accusizer 780; Particle Sizing Systems, Santa Barbara, CA, USA).

2.2. Cell culture

N_2A cell lines were obtained from the National Cancer Institute and ATCC (American Type Culture Collection), and maintained in DMEM, 10% fetal bovine serum under 5% CO_2. N_2A cells were seeded on coverslips coated with 0.1 mg/ml polylysine solution at $4 \times l0^5$ cells/ml and cultured within a 6-well microplate in the cell culture medium at 37 °C for 48 h. About the rat hippocampal neurons, the pregnant Sprague-Dawley rats for 18 days were sacrificed after anesthetized and disinfected. The fetal rats were taken from the abdominal cavity and the hippocampus tissue was separated. Next, hippocampus tissue was cut into fragments and digested by 0.125% trypsin at 37 °C for 15 min. The digestion product was centrifuged at 1000 r/min for 5 min, and the hippocampal neuron cells were resuspended. 4×10^5 cells were seeded in a 6-well culture plate which contains coverslips coated with polylysine. Cells were cultured in an incubator at 37° C and under 5% CO_2.

2.3. Binding of targeted MBs with cells

Static binding of MBs to N_2A cells was examined. Briefly, 1×10^8 PTMB or non-targeted IgG-MBs (NTMB) were added and incubated with the N_2A cells for 5 min (gently rotating the plate during the incubation period) and free MBs that did not attach to the cells were removed by a PBS rinse. The binding capability of PTMB or NTMB with cells was examined under a microscope.

2.4. US stimulation system and calcium fluorescence imaging

In order to perform live-cell fluorescence imaging of N_2A cells stimulated by US, an US stimulation system was built onto the Leica TCS SP5 laser-scanning confocal microscope. Briefly, one steel concave cell holder was first made, with a 2.0 × 3.5 cm hole in the middle. A coverlid could be placed to cover the hole (Fig. 1A). A single element US transducer with 2 MHz centre frequency was fabricated according to the previous report [16]. The US transducer was fixed on a self-made fixture, with a 45° angle to irradiate the cells cultivated on the glass coverlid (Fig. 1A). The distance between the transducer and the cells is about 10 mm. Then the self-made fixture of cell coverslips was fixed on a custom built-stage on a Leica TCS SP5 laser-scanning confocal microscope (Leica, Germany) (Fig. 1B).

Live-cell Ca^{2+} fluorescence imaging was carried out on the Leica TCS SP5 confocal microscope to monitor the cytoplasmic Ca^{2+} elevations elicited by US in N_2A cells. A calcium indicator, Fluo-4 AM, was used for the fluorescence imaging. Briefly, 91 μL 20% Pluronic F-127 in DMSO (Sigma, USA) was added into a vial containing 50 μg Fluo-4 AM, then 5 μL dye solution was diluted with 1 mL HBSS. 500 μL diluted solution was added to the surface of slices with cells. The cells were incubated at room temperature for 30 min and then washed with PBS. Fluo-4 AM can easily enter cells and be hydrolyzed into Fluo 4 by intracellular esterase. Upon Fluo-4 bind with the calcium ions, the green fluorescence would emit. To detect the fluorescence, 488 nm laser beam of an argon laser was delivered to those cells for excitation of Fluo-4 after passing through an excitation pinhole, galvo-mirror, a dichroic mirror, and a ×20 microscope objective. The light emitted from the cells was then collected by the same objective and recorded in a photomultiplier tube (PMT) detector via an emission pinhole, which allowed the selection of proper emission wavelengths. Time-series fluorescence images were acquired. The whole US stimulation and imaging system was illustrated as Fig. 1C, composed of a function generator, power amplifier and a transducer. An example low-intensity US stimulus waveform is illustrated to highlight the parameters used in their construction (Fig. 1D). US beam was transmitted from remotely positioned tissue-matched piezoelectric transducers. The distribution profiles of sound field was showed in Fig. 1E, revealing a 4 mm diameter cycle-shape acoustic field.

2.5. Generation and characterization of US waveforms

We constructed US waveforms by repeating US tone bursts. 2 MHz sinusoidal bursts were supplied from a function generator (AFG3102C, Tektronix, USA) to the transducer, followed by a 50-dB power amplifier (325LA, EI, USA). The peak-to-peak (Vpp) voltages of the input bursts were adjusted to 12, 21, 38 and 56 V. Our primary acoustic waveform had the following properties: f = 2 MHz, Pulse Width/T1 = 500 μs, Pulse Interval/T2 = 1 ms, Stimulus Duration T3 = 300 ms, Stimulus Interval/T4 = 3 s.

To characterize acoustic power levels, we recorded voltage waveforms produced by acoustic pressure waves using a hydrophone (ModelUMS3s/Nums3o32, the UK) and a digital oscilloscope (DSO-X 3024A, Agilent, USA). All pressure waves produced by US waveforms were measured at points corresponding to the position of targeted cells by positioning the hydrophone face using a XYZ micromanipulator. The vertical distance between the hydrophone and the probe was about 10 mm. The scanning area of the hydrophone exceeded the area of radiation area of US. The probe continuously emitted pulse waves. Our primary acoustic waveform had the following properties: f = 2 MHz, Pulse Width/T1 = 500 μs, Pulse Interval/T2 = 1 ms, Stimulus Duration T3 = 300 ms, Stimulus Interval/T4 = 3 s. The position of cell coverslips in recording chambers was remains unchanged. The acoustic pressure (IPA) was calculated using published equations and technical standards established by the American Institute of Ultrasound in Medicine and the National Electrical Manufacturers Association [17].

2.6. Temperature measure

Temperature was measured in the US focal zone using a Digital RTD/Thermocouple Thermometer/Data Logger (HH806, Omega, ENGLAND). The probe was placed in the focal zone of the US beam near the surface of coverslips with the presence of MBs.

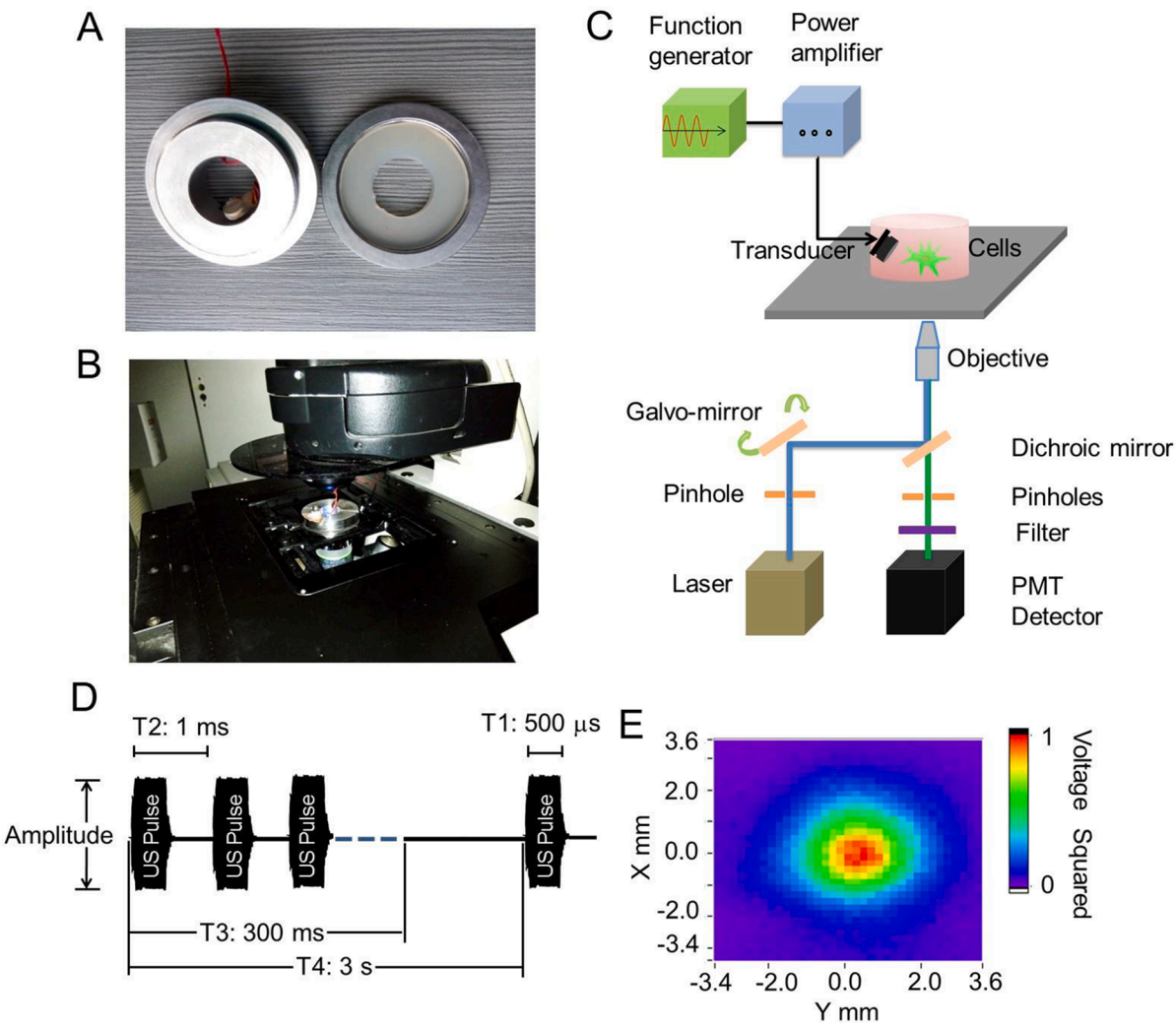

Fig. 1. US stimulation system and live cell calcium fluorescence imaging system. (A) One self-made steel cell holder and coverlid was designed for US stimulation, in which a 2 MHz ultrasonic transducer was fixed on the wall of holder. A 2.0 × 3.5 cm hole which can be cover by a glass coverlid was design in the middle to allow the light through the cell holder. Cells can be cultured on the glass coverlid and be irradiated by US. (B) Cell holder and coverlid can be built into a fixture with the cultivated cells and placed on a confocal microscope, thus building a live cell calcium fluorescence imaging system. (C) The diagram of whole US-stimulation live cell calcium fluorescence imaging system. (D) Characterization of US waveforms. (E) The acoustic field distribution scanned by acoustic field scanning system.

2.7. Treatment with inhibitors and GsMTx-4

To investigate the dependence of US-mediated Ca^{2+} elevation on calcium influx across the plasma membrane, the following approaches including elimination of extracellular calcium and blocking of ion channels in the cell membrane were used: (i) 5 mM EDTA was added to cell culture medium for 20 min to eliminate extracellular calcium from the medium. (ii) N_2A or primary hippocampal neurons were treated with 3 μM GsMTx-4 (Tocris) for 30 min to block Piezo1 channel. (iii) N_2A or primary hippocampal neurons were treated with 150 μM $CdCl_2$ (Aladdin) for 10 min to block the cation channels on cell membrane.

2.8. Data analysis

Confocal images were analyzed offline using LAS AF Lite software. The changes in green fluorescence of Fluo 4 were expressed as dF/F_0 calculated through standard approaches, where $dF = F\text{-}F_0$. Temporal changes of the mean fluorescence in targeted cells were then analyzed. The max dF/F_0 of cells were compared. Average data were presented in a bar diagram as a mean ± SEM of indicated sample sizes. Two-tail unpaired Student *t* test or one-way ANOVA and Fisher least significant difference (LSD) was used to determine the statistical significance. *P < 0.05, **P < 0.001, ***P < 0.0001, considered statistically significant. The number of invading cells was quantitated from triplicate experiments.

3. Results

3.1. Cytoplasmic Ca^{2+} variations in N_2A cells elicited by US

To determine if US irradiation can activate Ca^{2+} transients, N_2A cells seeded on the glass coverlid put into the mixture were exposed to US at different acoustic pressure. Results showed a significantly elicited fluorescence increases were observed in N_2A cells after immediate US stimulation, and the fluorescence intensity decayed after 5 min (Fig. 2A). In the cells exhibiting calcium elevations, PI positive cells were rarely, indicating that US irradiation did not result in cell death and Ca^{2+} influx did not result from the increase of cell membrane permeability. By contrast, the fluorescence intensity did not change in the N_2A cells which did not receive US irradiation. Ca^{2+} influx into the cytoplasm of N_2A cells along with time was quantitated using the relative fluorescence intensity dF/F_0, illustrating the Ca^{2+} instantaneous elevation in N_2A cells occurred immediately post US irradiation, reached a peak after 10 s and gradually reduced within 2 min (Fig. 2B). Transient

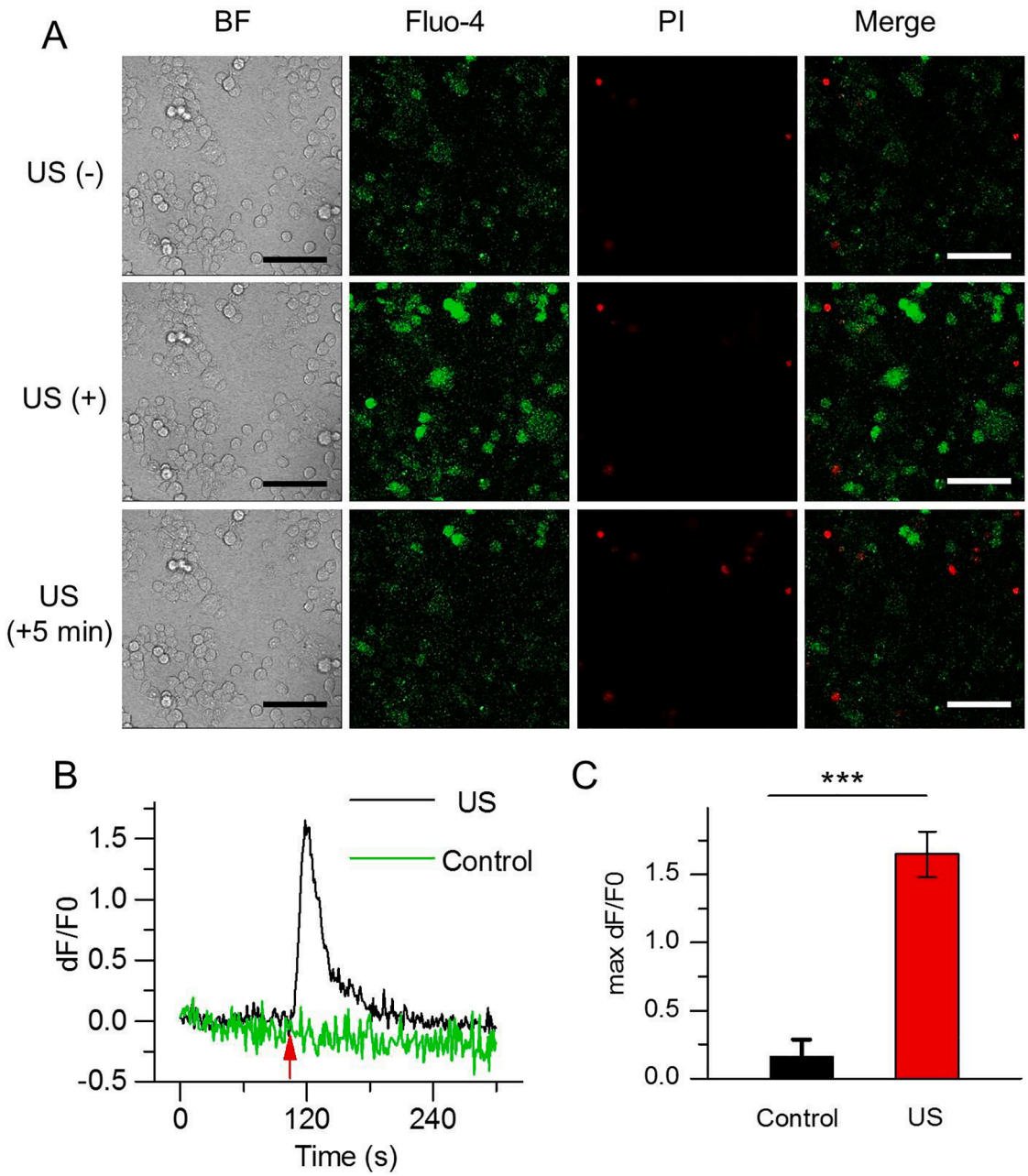

Fig. 2. US triggers Ca^{2+} transients in N_2A. (A) Confocal images of N_2A cells before, immediately or 5 min after receiving US irradiation in bright field, Fluo-4 AM (green), PI staining (red) and merge model. The fluorescence intensity of Fluo-4 reflects the concentration of intracellular calcium. PI can stain dead cells red due to cell membrane destruction. Scale bar, 100 μm. (B) Significantly enhanced Ca^{2+} fluorescence signals (dF/F_0) could be immediately observed in N_2A cells in response to US stimulation and trended to decay after 5 min. (C) Average maximum dF/F_0 mean fluorescence intensity in control and US-stimulated cells. (C) Data are expressed as mean ± SEM and analyzed by two-tail unpaired Student *t* test. ***$P < 0.0001$ vs Control. (n = 46 cells from 3 slices). n represents the number of cells with the enhanced Ca^{2+} signals. Acoustic pressure is 0.17 MPa, T1 = 500 μs, T2 = 1 ms, T3 = 300 ms, T4 = 3 s, total time is 10 s. (For interpretation of the references to colour in this figure legend, the reader is referred to the web version of this article.)

calcium elevations were not observed in the N_2A cells that did not receive US treatment. The maximum average fluorescence intensity from US-irradiated N_2A cells was 1.65 ± 0.17, approximately 10-fold higher than these N_2A cells that did not receive US treatment (DF/F_0 = 0.16 ± 0.13, Fig. 2C).

3.2. *Intensity-dependent US effect on cytoplasmic Ca^{2+} elevation in N_2A*

Next, we further examined the effect of US intensity on cytoplasmic Ca^{2+} elevation. A series of different acoustic pressures from 0.03 MPa to 0.17 MPa was used for irradiate the N_2A cells. Fig. 3A showed that fluorescence intensity of N_2A cells increased with increasing acoustic pressures. At 0.03 MPa acoustic pressure, the fluorescence intensity of N_2A cells did not increase, with 0.03 ± 0.03 baseline fluorescence intensity. At 0.06 MPa acoustic pressure, fluorescence intensity slightly increased to 0.09 from baseline (acoustic pressure = 0.03 MPa). In contrast, the fluorescence intensity at the simulated acoustic pressures of 0.11 and 0.17 MPa significantly increased to 0.68 ($p < 0.001$) and 1.48 ($p < 0.0001$), respectively (Fig. 3B and 3C). Together, these results indicate that there is an intensity-dependent response between fluorescence intensity and acoustic pressures in N_2A. To test whether these cells can repeatedly be in response to US excitation, the N_2A cells was

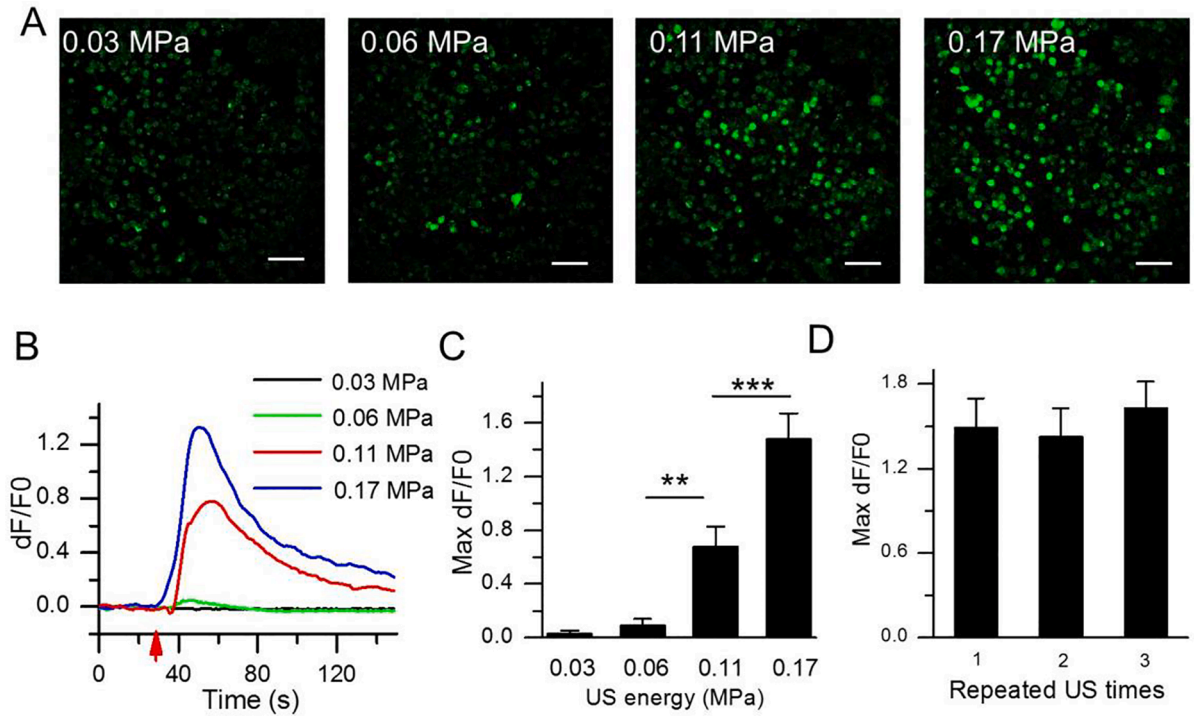

Fig. 3. Intensity-dependent cytoplasmic Ca^{2+} elevation in N_2A. (A) Confocal images of N_2A cells receiving various acoustic pressures at 0.03, 0.06, 0.11 or 0.17 MPa, showing an US intensity-dependent cytoplasmic Ca^{2+} elevation. Scale bar, 100 μm. (B) Temporal fluorescence intensity curves in N_2A cells at different acoustic pressures. (C) Analysis of Fluo-4 mean fluorescence intensity at different acoustic pressures. (n = 60 cells from 3 slices). (D) Ca^{2+} transients can response to the repeated US stimulation at 0.17 MPa acoustic pressure (n = 37 cells from 3 slices). Data are expressed as mean ± SEM and analyzed by one-way ANOVA and Fisher least significant difference (LSD). ***$P < 0.0001$, **$P < 0.001$. n represents the number of invading cells. T1 = 500 μs, T2 = 1 ms, T3 = 300 ms, T4 = 3 s, total time is 10 s.

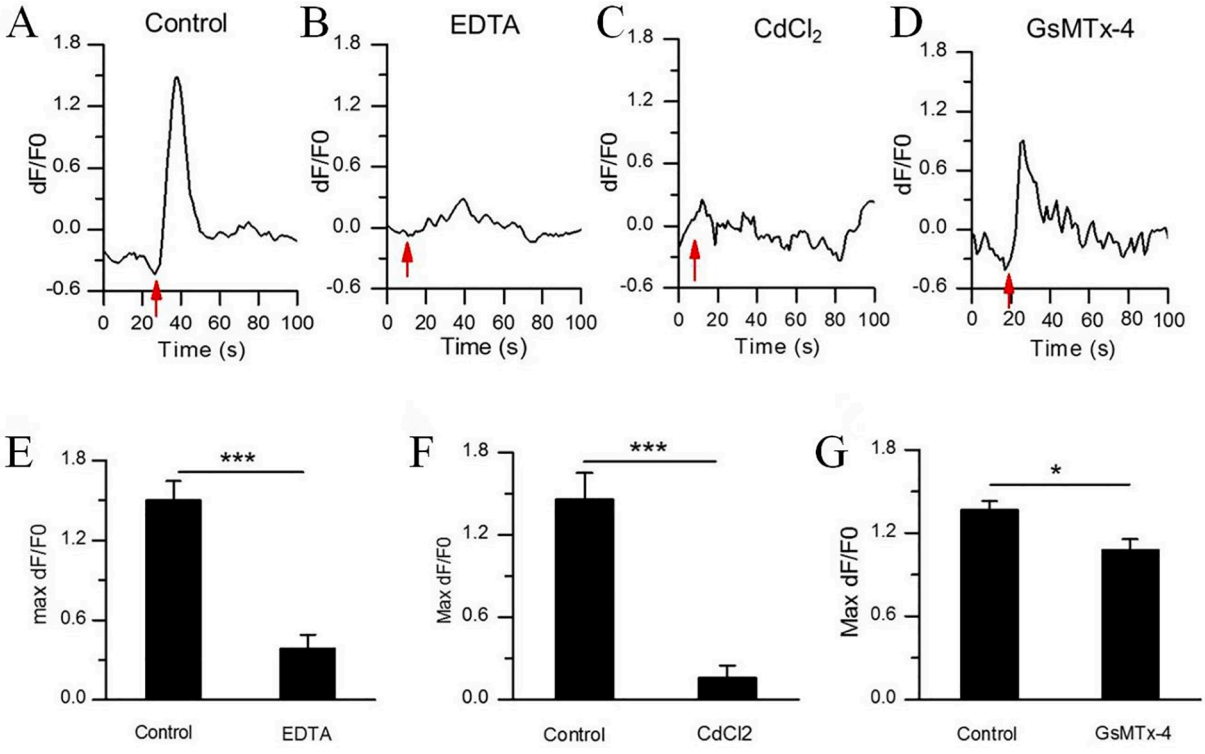

Fig. 4. Characteristics of US-evoked Ca^{2+} transients in N_2A. (A-D) Representative traces of US-activated Ca^{2+} fluorescence signals of N_2A cells treated with PBS control, EDTA, $CdCl_2$ or GsMTx-4 inhibitors. (E-G) The average maximum dF/F_0 of N_2A cells treated with (E) 5 mM EDTA (n = 60 cells from 3 slices), (F) 150 μM $CdCl_2$ (n = 79 cells from 3 slices), or (G) 3 μM GsMTx-4 (n = 64 cells from 3 slices). Bars represent the mean ± SEM. Two-tail unpaired Student *t* test, ***$P < 0.0001$, **$P < 0.001$, *$P < 0.05$. n represents the number of invading cells. Acoustic pressure is 0.17 MPa, T1 = 500 μs, T2 = 1 ms, T3 = 300 ms, T4 = 3 s, total time is 10 s.

irradiated for three repeated US stimulation at 5 min interval. We observed that the maximum fluorescence intensity from the 1st, 2nd and 3rd US irradiation were 1.49, 1.42, 1.63, respectively ($p > 0.05$), suggesting that Ca^{2+} transients could be repeatedly observed by repeated US stimuli (Fig. 3D).

3.3. Contributors to the US-activated Ca^{2+} transients in N_2A

To confirm the contributors which lead to the cellular Ca^{2+} elevation, EDTA (5 mM) was used to incubate with N_2A to chelate the extracellular Ca^{2+}. Interestingly, calcium chelation by EDTA significantly inhibited the cellular Ca^{2+} elevation in N_2A (Fig. 4B and E) induced by US, with 0.38 ± 0.10 fluorescence intensity vs 1.50 ± 0.15 (control) (***P < 0.0001). Addition of the cell membrane cationic channels blockers nearly abolished Fluo-4 signals in response to US, control: 1.46 ± 0.19 vs $CdCl_2$: 0.16 ± 0.09 (***P < 0.0001) (Fig. 4C and F). After wash-off with PBS, the inhibition effect of $CdCl_2$ was able to be partly reversed, reaching 0.82 ± 0.17 fluorescence intensity (*P < 0.05, vs $CdCl_2$: 0.16 ± 0.09) (Fig. 8A). Next, we tested the Piezo1 inhibitor peptide, GsMTx-4, revealing 3 μM of GsMTx-4 reduced the amplitude of the cellular Ca^{2+} elevation in N_2A cells (Fig. 4D and G). (1.36 ± 0.06 for control vs. 1.08 ± 0.07 for GsMTx-4) (*P < 0.05).

The previous data showed US only with appreciate irradiation (>0.11 MPa) can activate the extracellular Ca^{2+} influx into N_2A and lead

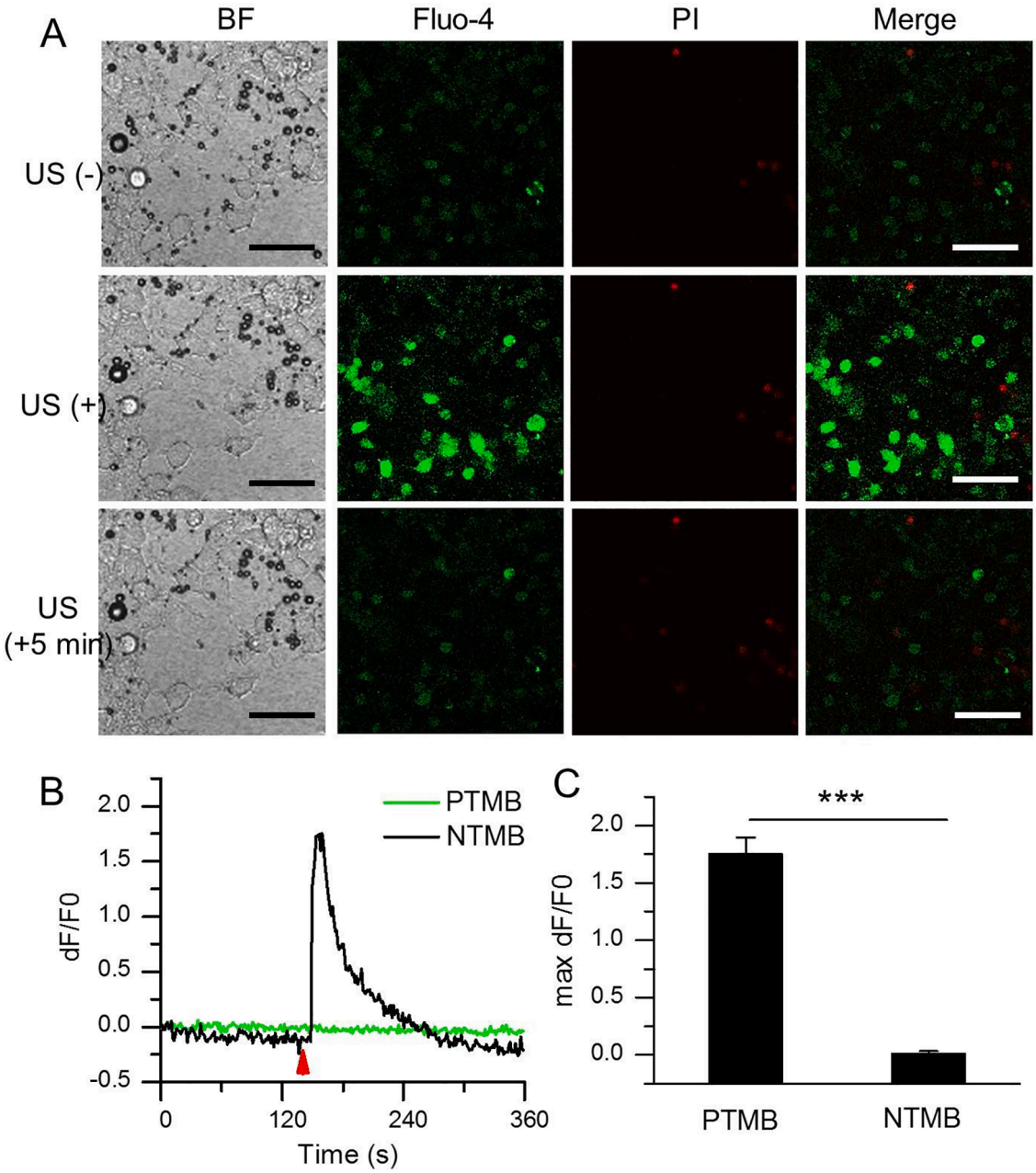

Fig. 5. Piezo1-MBs sensitized the effect of US stimulation of N_2A. (A) Confocal images of PTMB-binding N_2A cells before, immediately or 5 min after receiving US irradiation in bright field, Fluo-4 AM (green), PI staining (red) and merge model. Acoustic pressure is 0.03 MPa, T1 = 500 μs, T2 = 1 ms, T3 = 300 ms, T4 = 3 s, total time is 5 s. Scale bar, 100 μm. (B) Temporal fluorescence intensity changes of Piezo1-MBs-binding N_2A cells before, immediately or 5 min after receiving US irradiation. (C) Average maximum dF/F_0 of N_2A cells incubated with the NTMB (n = 189 cells from 3 slices) or the adhered PTMB (n = 292 cells from 3 slices), followed by US irradiation. Acoustic pressure is 0.03 MPa, T1 = 500 μs, T2 = 1 ms, T3 = 300 ms, T4 = 3 s, total time is 5 s. Data are expressed as mean ± SEM. ***P < 0.0001. (For interpretation of the references to colour in this figure legend, the reader is referred to the web version of this article.)

to the cellular Ca^{2+} elevation. However, it is inevitable to bring with some unexpected damages when using too high US intensity. Also, heating effect from US irradiation possibly occurs. A lower US intensity is desirable, especially for long duration US exposure. Since evidences have demonstrated that US can promote the extracellular Ca^{2+} influx via Piezo1 protein, a mechanical ion channel. Considering that MBs are sensitive to US, we incubated PTMB with N_2A cells. As expected, PTMB could be bound to the surface of N_2A (Fig. 5A, BF). It is notable that US irradiation at 0.03 MPa acoustic pressure (an US intensity did induce any extracellular Ca^{2+} influx) could not destruct these bubbles, but apparently activate Ca^{2+} transients of N_2A cells (Fig. 5A, Fluo-4; Supplementary Video 1). PI-positive cells were few (Fig. 5A, PI). The fluorescence intensity change along with time showed a sharp elevation of Fluo-4 signals in N_2A cells with PTMB after US stimulation. By contrast, fluorescence signal intensity did not change in these N_2A cells with NTMB. (Fig. 5B). The maximum fluorescence signal intensity for N_2A cells with PTMB achieved 1.75 ± 0.15 DF/F_0, significantly higher than these cells with NTMB (Fig. 5C). The addition of EDTA (5 mM; 20 min), $CdCl_2$ (150 μM; 10 min), GsMTx-4 (3 μM; 30 min) led to a significant reduction of the Ca^{2+} signal in the US-stimulated N_2A cells, with 0.37 ± 0.12, 0.19 ± 0.04 or 1.09 ± 0.10 maximum fluorescence signal intensity for EDTA, $CdCl_2$ or GsMTx-4 treatment, respectively(Fig. 6).

Next, we further examined whether PTMB enhanced US-stimulated Ca^{2+} transients can occur in neuron cells. The rat hippocampal neurons were isolated from newborn rat brain and cultivated on the glass coverlid fixed in the self-made mixture and then incubated with PTMB. After washing out these unbound bubbles, these neuron cells were exposed to US at 0.03 MPa acoustic pressure. Fig. 7D illustrates the Ca^{2+} temporal variations in neurons with PTMB and NTMB. Obviously, neurons with PTMB clearly exhibited transient Ca^{2+} elevations when US was on (DF/F_0 = 1.52 ± 0.19, Fig. 7E; Supplementary Video 2). In contrast, transient calcium elevation was not observed in NTMB group (DF/F_0 = 0.05 ± 0.04, Fig. 7E). Interestingly, the level of calcium elevation was dependent on the bubble number bound on the surface of cells. The average maximum relative fluorescence intensity of neuron cells was 0.52 ± 0.10 for 3 adhered bubbles, 0.92 ± 0.15 for 5 adhered bubbles, 1.47 ± 0.18 for 7 adhered bubbles when using the same 0.03 MPa acoustic pressure, respectively (Fig. 7F).

4. Discussion

Several investigations have demonstrated that US can modulate neuronal activity by enhancing and/or suppressing the amplitudes and/or conduction velocities of evoked nerve potentials. Tyler et al found that US of low intensity and 0.44–0.67 MHz can elicit neuronal action potential and trigger the release of synaptic vesicles to mediate synaptic conduction [11]. Shung found that US can activate Ca^{2+} transients in human umbilical vein endothelial cells [18] and cancer cells [19]. Jan et al found that the current of Nav1.5 mechanically sensitive sodium channels and dual-channel potassium channels (K_2P) increased by 23% through the detection of patch clamps with stimulation of focused US (10 MHz, 0.3–4.9 W/cm^2) [20]. In our study, we observed that US exposure can induce an increase in the internal Ca^{2+} concentration of N_2A and neurons. More importantly, we confirmed the targeted MBs adhered to Piezo1 can further enhance these neural cells responsiveness to US stimulation.

Piezo1 is a mechanosensitive ion channel (MSC) discovered by Coste et al in mouse N_2A neuronal tumor cells [13], containing 2100 ~ 4700 amino acids with 24 ~ 40 transmembrane domains which forms a trimeric propeller-like structure. The extracellular domains resembling

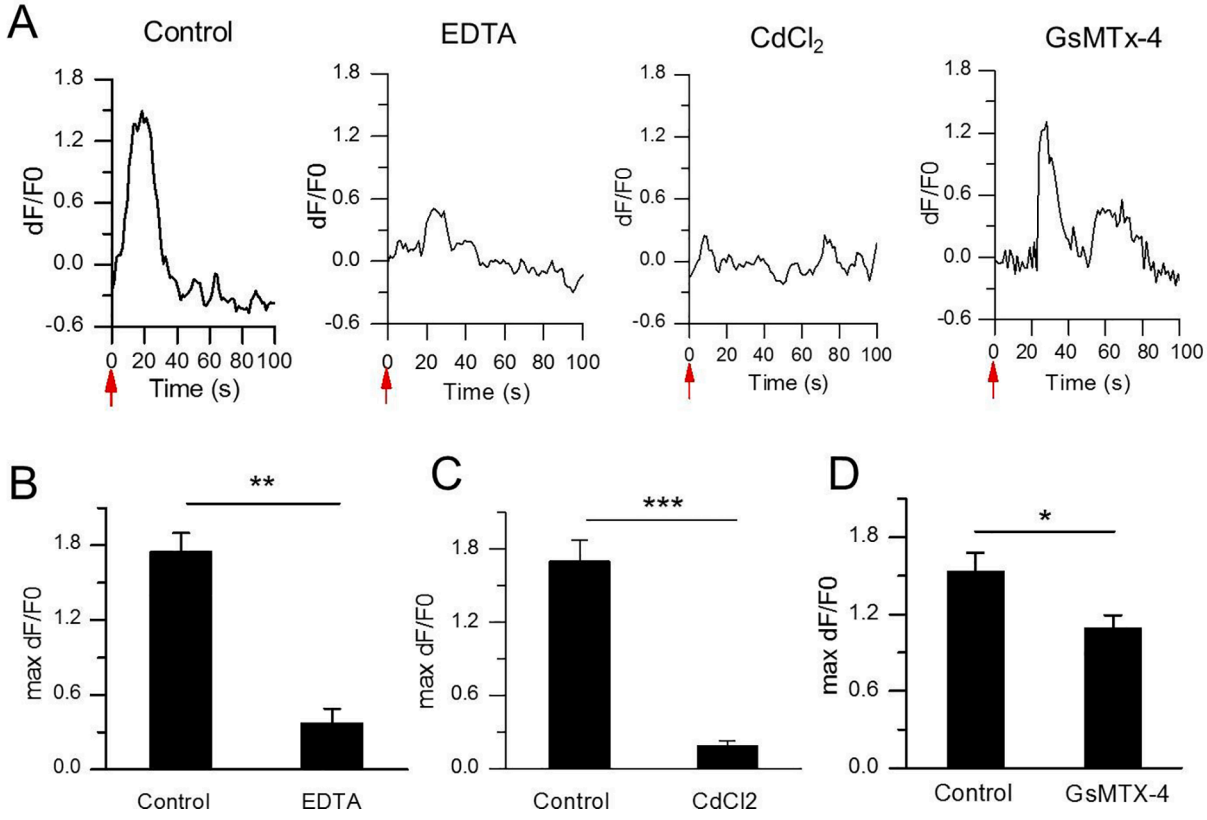

Fig. 6. Characteristics of US-evoked Ca^{2+} transients in N_2A with the adhered PTMB. (A) Representative traces of US-activated Ca^{2+} fluorescence signals of PTMB-binding N_2A cells treated with PBS control, EDTA, $CdCl_2$ or GsMTx-4 inhibitors. Acoustic pressure is 0.03 MPa, T1 = 500 μs, T2 = 1 ms, T3 = 300 ms, T4 = 3 s, total time is 5 s. (B-D) The average maximum dF/F_0 of N_2A cells treated with (B) 5 mM EDTA (n = 292 cells from 3 slices), (C) 150 μM $CdCl_2$ (n = 152 cells from 3 slices) or (D) 3 μM GsMTx-4. (n = 80 cells from 3 slices). Bars represent the mean ± SEM and analysed by two-tail unpaired Student *t* test. ***$P < 0.0001$, **$P < 0.001$, *$P < 0.05$.

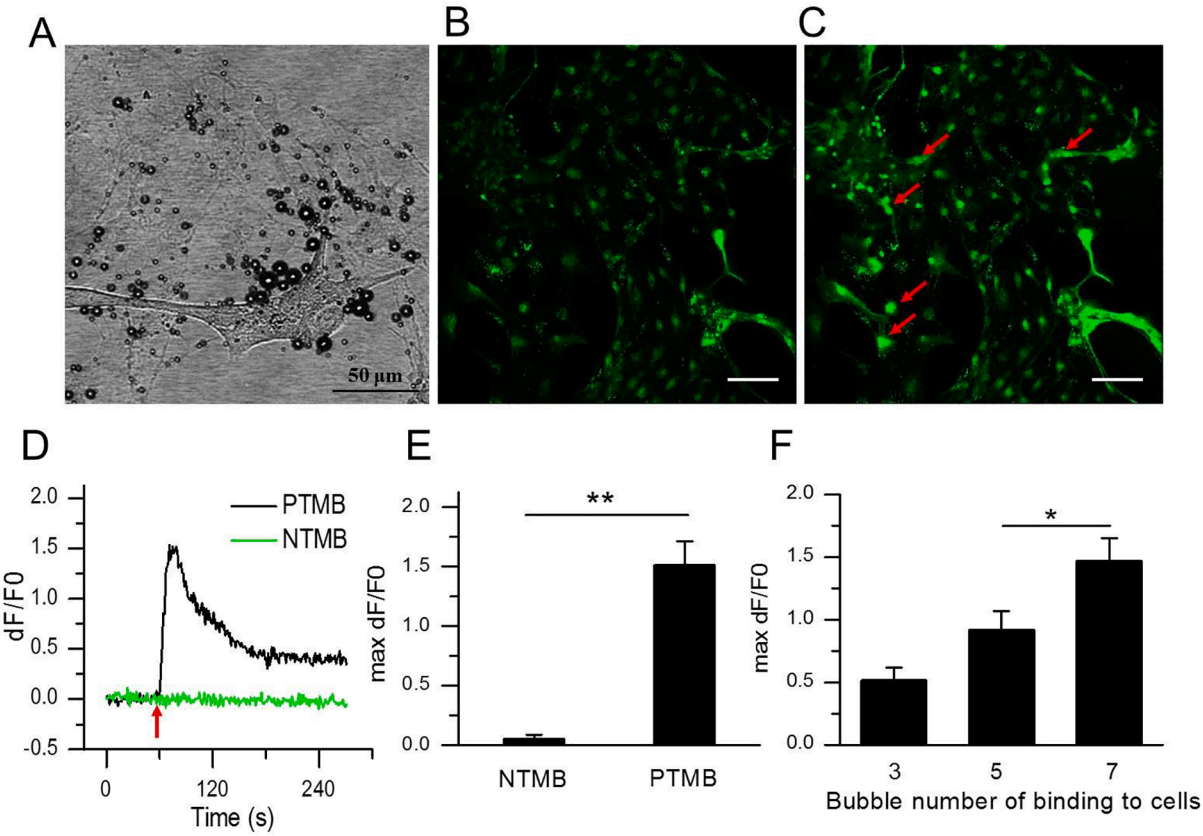

Fig. 7. PTMB sensitized the effect of ultrasonic stimulation of neurons. (A) Bright field image of rat primary hippocampal neurons bound with Piezo1-MBs before US irradiation. (B) Confocal image of PTMB-binding hippocampal neurons stained with Fluo-4 AM before US irradiation. (C) Confocal image of PTMB-binding hippocampal neurons stained with Fluo-4 AM immediately after US irradiation. Acoustic pressure is 0.03 MPa, T1 = 500 μs, T2 = 1 ms, T3 = 300 ms, T4 = 3 s, total time is 5 s. Scale bar, 100 μm. (D) Temporal fluorescence intensity changes of hippocampal neurons in NTMB and PTMB groups. (E) Average maximum dF/F_0 of hippocampal neurons in NTMB (n = 86 cells from 3 slices) and PTMB (n = 160 cells from 3 slices) groups. (F) Average maximum dF/F_0 of hippocampal neurons binding with 3 (n = 93 cells from 4 slices), 5 (n = 74 cells from 4 slices), 7 (n = 95 cells from 4 slices) PTMB, respectively. Data are expressed as mean ± SEM and analysed by two-tail unpaired Student *t* test or one-way ANOVA. $^{**}P < 0.001$, $^{*}P < 0.05$.

three distal blades and a central cap. The transmembrane region forms three peripheral wings and a central pore module that encloses a potential ion-conducting pore. The rather flexible extracellular blade domains are connected to the central intracellular domain by three long beam-like structures. As the main mechanical receptors, MSCs can convert the mechanical stimulation from the surface of cells into intracellular electrical signals or chemical signals.

MBs are ball-shape phospholipid particles filled with perfluoropropane, with 1 μm average particle size (Fig. 8B). They possess a significantly higher sensitivity to the US than cells [21]. In our study, we successfully fabricated the PTMB and bind them to the N_2A cells via antigen–antibody linkage. As expected, a strong US-stimulated Ca^{2+} transients was produced in these MBs-adhered N_2A cells at 0.03 MPa acoustic pressure. By contrast, US-stimulated Ca^{2+} transients did not

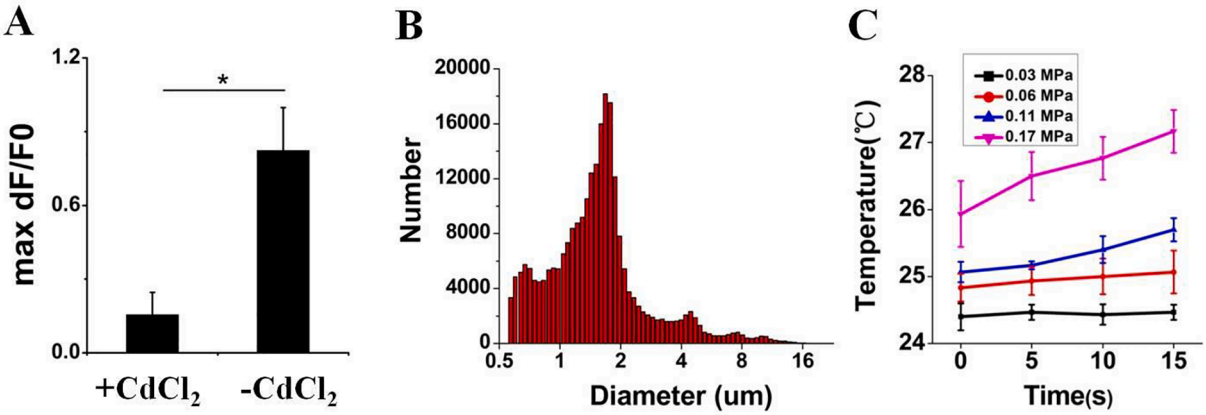

Fig. 8. (A) The average maximum dF/F_0 of N_2A cells after wash-off with PBS. Bars represent the mean ± SEM. Two-tail unpaired Student *t* test, $^{*}P < 0.05$. Acoustic pressure is 0.17 MPa, T1 = 500 μs, T2 = 1 ms, T3 = 300 ms, T4 = 3 s, total time is 10 s.(B) The size distributions of targeted MBs. (C) Temperature of the US focal zone.

occur at that acoustic pressure for those plain N_2A cells. Also, we found that PTMB can sensitise the effect of US on neurons from rat brains. Chelating extracellular calcium ions with EDTA can greatly diminished the Ca^{2+} response, showing that extracellular Ca^{2+} was highly involved in US-mediated calcium transients of N_2A. Inhibitors such as $CdCl_2$ greatly inhibit the response to US, suggesting that calcium transients was mainly mediated by cationic channels on the membrane of N_2A. Notably, GsMTx-4, a specific blocker of Piezo1 [22] partly inhibited US-mediated calcium transients of N_2A, showing that other cationic channels was probably involved in US-induced Ca^{2+} elevations as well.

In the past years, there are some preliminary studies about the biophysical mechanism of ultrasonic neuromodulation. Burks found that pulsed focused ultrasound (pFUS) acoustic radiation forces mechanically activate a Na^{+}-containing TRPC1 current upstream of VGCC rather than directly opening VGCC in kidney and skeletal muscle. The electrogenic function of TRPC1 provides potential mechanistic insight into other pFUS techniques for physiological modulation and optimization strategies for clinical implementation [23]. Tyler believed that US affects the viscoelasticity of neuronal cell membranes and extracellular fluids, altering action potentials and cell membrane conductivity through voltage-gated ion channels and mechanical-sensitive receptors [24]. He pointed out that the radiation force, microstreaming, shockwave, and cavitation effect from US may be the potential mechanism of ultrasonic neuromodulation. Inertia cavitation lead to the resonation, expansion, and collapse of gas bubbles present in some biological tissue. These microexplosions can influence membrane porosity [25,26]. In general, when the acoustic pressure is less than 1 MPa, US can modulate neuronal activity, and there is no injury to cells by cavitation effect [27]. At the acoustic pressures used in our study, we did not observe membrane porosity from cavitation through PI staining. In the cells exhibiting calcium elevations by US and PTMB, few PI-positive cells were found. In addition, significant temperature increase ($<<1$ ℃) was not observed during US irradiation, as illustrated in Fig. 8C. Thus, we infer that the cytoplasmic calcium elevation was mainly caused by acoustic radiation force. PTMB which bind to the cells may provide higher sensitivity to US through pulling the Piezo 1, leading to the opening of Piezo1 channel. Still, there have some limitations in the study. The one is that some other channels would perhaps be opened due to the mechanotransduction from the US-exciting PTMB on the membrane. The other one is the difficulty for PTMB to bind with nerve cells in the in vivo condition because its microscale particle size limit them not to penetrate out of the blood vessels. To overcome it, nanobubbles would be needed to develop.

5. Conclusions

In this study, we fabricated PTMB which can bind to the N_2A cells and primary cultured neurons. In order to facilitate the manipulation of US stimulation on cultured cells and the observation of their calcium transients, we set up an in vitro US stimulation system which can fixed on a commercialized microscope. After examining the effects of US-stimulated calcium transients of N_2A cells, we confirmed the sensitized effect of PTMB on ultrasonic stimulation of N_2A cells and primary cultured neuronal cells. Our finding provides a safer and strategy for US neuromodulation in the future.

Declaration of Competing Interest

The authors declare that they have no known competing financial interests or personal relationships that could have appeared to influence the work reported in this paper.

Acknowledgements

The work was supported by the Ministry of Science and Technology Key Research and Development Plan of China (2018YFC0115900, 2020YFA0908800), National Natural Science Foundation of China (81871376), Guangdong Innovation Platform of Translational Research for Cerebrovascular Diseases, and Shenzhen Science and Technology Innovation Committee (Grant Nos. JCYJ20180507182420114, JCYJ20190812171820731 and ZDSYS201802061806314).

Appendix A. Supplementary data

Supplementary data to this article can be found online at https://doi.org/10.1016/j.ultsonch.2021.105494.

References

[1] C. Demene, J. Baranger, M. Bernal, C. Delanoe, S. Auvin, V. Biran, M. Alison, J. Mairesse, E. Harribaud, M. Pernot, M. Tanter, O. Baud, Sci. Transl. Med. 9 (2017) eaah6756.
[2] V. Cotero, Y. Fan, T. Tsaava, A.M. Kressel, I. Hancu, P. Fitzgerald, K. Wallace, S. Kaanumalle, J. Graf, W. Rigby, T.J. Kao, J. Roberts, C. Bhushan, S. Joel, T. R. Coleman, S. Zanos, K.J. Tracey, J. Ashe, S.S. Chavan, C. Puleo, Nat. Commun. 10 (2019) 952.
[3] A.R. Rezai, M. Ranjan, P.F. D'Haese, M.W. Haut, J. Carpenter, U. Najib, R.I. Mehta, J.L. Chazen, Z. Zibly, J.R. Yates, S.L. Hodder, M. Kaplitt, Proc. Natl. Acad. Sci. U S A. 117 (2020) 9180–9182.
[4] A. Alamri, I. Ughratdar, M. Samuel, K. Ashkan, Br. J. Neurosurg. 29 (2015) 319–328.
[5] M. van de Ruit, M.J. Perenboom, M.J. Grey, Brain. Stimul. 8 (2015) 231–239.
[6] C.K. Kim, A. Adhikari, K. Deisseroth, Nat. Rev. Neurosci. 18 (2017) 222–235.
[7] W.H. She, T.T. Cheung, C.R. Jenkins, M.G. Irwin, Hong Kong Med. J. 22 (2016) 382–392.
[8] S. Ibsen, A. Tong, C. Schutt, S. Esener, S.H. Chalasani, Nat. Commun. 6 (2015) 8264.
[9] W. Legon, T.F. Sato, A. Opitz, J. Mueller, A. Barbour, A. Williams, W.J. Tyler, Nat. Neurosci. 17 (2014) 322–329.
[10] W. Lee, H.C. Kim, Y. Jung, Y.A. Chung, I.U. Song, J.H. Lee, S.S. Yoo, Sci. Rep. 6 (2016) 34026.
[11] W.J. Tyler, Y. Tufail, M. Finsterwald, M.L. Tauchmann, E.J. Olson, C. Majestic, PLoS One. 3 (2008), e3511.
[12] A. Anishkin, S.H. Loukin, J. Teng, C. Kung, Proc. Natl. Acad. Sci. U S A. 111 (2014) 7898–7905.
[13] J.M. Bertrand Coste, M. Schmidt, T.J. Earley, S. Ranade, M.J. Petrus, A.E. Dubin, A. Patapoutian, Science 330 (2010) 55–60.
[14] J. Ge, W. Li, Q. Zhao, N. Li, M. Chen, P. Zhi, R. Li, N. Gao, B. Xiao, M. Yang, Nature 527 (2015) 64–69.
[15] Z. Qiu, J. Guo, S. Kala, J. Zhu, Q. Xian, W. Qiu, G. Li, T. Zhu, L. Meng, R. Zhang, H. C. Chan, H. Zheng, L. Sun, iScience. 21 (2019) 448–457.
[16] A. Atalar, V. Jipson, A.R. Koch, C.F. Quate, Annu. Rev. Mater. Res. 9 (1979) 255–281.
[17] G.R. Harris, Ultrasound Med. Biol. 11 (1985) 803–817.
[18] J.Y. Hwang, H.G. Lim, C.W. Yoon, K.H. Lam, S. Yoon, C. Lee, C.T. Chiu, B.J. Kang, H.H. Kim, K.K. Shung, Ultrasound Med. Biol. 40 (2014) 2172–2182.
[19] J.Y. Hwang, N.S. Lee, C. Lee, K.H. Lam, H.H. Kim, J. Woo, M.Y. Lin, K. Kisler, H. Choi, Q. Zhou, R.H. Chow, K.K. Shung, Biotechnol. Bioeng. 110 (2013) 2697–2705.
[20] J. Kubanek, J. Shi, J. Marsh, D. Chen, C. Deng, J. Cui, Sci. Rep. 6 (2016) 24170.
[21] L. Meng, F. Cai, P. Jiang, Z. Deng, F. Li, L. Niu, Y. Chen, J. Wu, H. Zheng, Appl. Phys. Lett. 104 (2014) 31–34.
[22] R. Gnanasambandam, C. Ghatak, A. Yasmann, K. Nishizawa, F. Sachs, A. S. Ladokhin, S.I. Sukharev, T.M. Suchyna, Biophys. J. 112 (2017) 31–45.
[23] Scott R. Burks, Rebecca M. Lorsung, Matthew E. Nagle1, Tsang-Wei Tu, and Joseph A. Frank. Theranostics. 9 (2019) 5517–5531.
[24] W.J. Tyler, Neuroscientist 17 (2011) 25–36.
[25] A. Shi, P. Huang, S. Guo, L. Zhao, Y. Jia, Y. Zong, M. Wan, Ultrason. Sonochem. 31 (2016) 163–172.
[26] S. Bian, A. Seth, D. Daly, R. Carlisle, E. Stride, Rev. Sci. Instrum. 88 (2017), 034302.
[27] D. Dalecki, Annu. Rev. Biomed. Eng. 6 (2004) 229–248.